JACS
JOURNAL OF THE AMERICAN CHEMICAL SOCIETY

COMMUNICATION

pubs.acs.org/JACS

Preparation of Water-Soluble Magnetic Nanocrystals Using Aryl Diazonium Salt Chemistry

Nébéwia Griffete,[†] Frédéric Herbst,[†] Jean Pinson,[‡] Souad Ammar,[†] and Claire Mangeney*[,†]

[†]ITODYS, Université Paris Diderot-Paris 7 (UMR CNRS 7086), 15 rue Jean de Baïf, 75013 Paris, France

[‡]Physico-Chimie des Electrolytes, des Colloïdes et Sciences Analytiques, ESPCI ParisTech, CNRS UMR 7195, 10 rue Vauquelin,75231 Paris Cedex 05, France

Supporting Information

ABSTRACT: A novel and facile methodology for the *in situ* surface functionalization of Fe_3O_4 nanoparticles is proposed, based on the use of aryl diazonium salts chemistry. The grafting reaction involves the formation of diazoates in a basic medium. These species are unstable and dediazonize along a homolytic pathway to give aryl radicals which further react with the Fe_3O_4 NPs during their formation and stop their growth. Advantages of the present approach rely not only on the simplicity, rapidity, and efficiency of the procedure but also on the formation of strong Fe_3O_4—aryl surface bonds, highly suitable for further applications.

Magnetic nanoparticles (NPs) have been the subject of extensive research during the past decade because of their potential applications in many fields, such as magnetic ferrofluids,[1] contrast agents for magnetic resonance imaging,[2] NPs/ligand targeting systems for drug delivery,[3] catalysis, or Forward osmosis processes for water treatment.[4] One difficulty, however, with such nanomaterials is to control their dispersion in an organic or aqueous medium, and it is usually necessary to functionalize the nanoparticles in order to ensure effective control over the colloidal stability. Toward this end, various organic ligands have been used: carboxylates,[5] amines or diols,[6] phosphates and phosphonates,[7] and sulfonates and thiols.[8] Although effective in several nonaqueous environments, these anchoring groups of the chelate type often fail on metal oxide surfaces in aqueous or protic media due to the hydrolytic instability of the surface attachment and/or the dynamic nature of the interaction. Therefore, developing efficient functionalization strategies for obtaining strong and stable linkages between the iron oxide NP surface and the organic coating still remains challenging.

In this paper, we address this issue by proposing a novel and facile methodology for the *in situ* surface functionalization of Fe_3O_4 nanoparticles, based on the use of diazonium salts chemistry. Aryl diazonium salts have been shown recently to be useful organic agents for the surface modification of carbon-based[9] and metallic[10] (gold, platinum, palladium, ruthenium, and titanium) nanoparticles, affording strong carbon or metal—carbon linkages. The mechanism of these grafting reactions relies on the reduction of the diazonium salt (by the surface to be modified or by a reducing agent in solution) generating aryl radical species that bind to the metal surface. In spite of the fact that grafting of diazonium on oxide surfaces has already been reported,[11] such unique chemistry has never been extended to the functionalization of oxide nanoparticles, probably due to the poor reducing character of this type of material.

In this paper, we circumvented this difficulty by taking advantage of the transformation of diazonium species to diazoates in basic media. Indeed, hydroxyl ions react with diazonium salts to give transient diazohydroxides, which are deprotonated to diazoates.[12] The latter are unstable and dediazonize spontaneously to give aryl radicals. These radicals were shown recently to react with iron or gold surfaces.[13] If they are present during the synthesis of Fe_3O_4 NPs, these aryl radicals should give NPs modified with aryl groups through covalent linkages, affording a highly stable anchoring of the organic coating at the surface of the NPs.

As a proof of concept, we studied the hydrolysis of iron chloride salts in an alkaline aqueous solution (pH = 9) in the presence of the diazonium salt 2-hydroxyethylphenyldiazonium tetrafluoroborate (BF_4,N_2-C_6H_4-$(CH_2)_2$-OH) resulting in the formation of iron oxide magnetite Fe_3O_4 coated by aryls with carbon—surface covalent bonds, as schematized in Figure 1. The aryl-coated NPs (NP-C_6H_4-$(CH_2)_2$-OH) were characterized by Transmission Electron Microscopy (TEM), Thermal Gravimetric Analysis (TGA), and InfraRed (IR) spectroscopies as well as through their magnetic properties.

BF_4, N_2-C_6H_4-$(CH_2)_2$-OH was synthesized following a procedure described in the literature.[14] Concerning the Fe_3O_4 nanoparticles, they were synthesized as follows: in a typical reaction, 2.9 mmol of $FeCl_3$ and 1.2 mmol of $FeSO_4$ were dissolved in 5 mL of deionized water. The solution was purged with nitrogen, and the inert atmosphere was maintained for the duration of the synthesis. Then 3 mL of NaOH (c = 1 M) were rapidly added under vigorous stirring. The color of the solution changed immediately from yellow to dark, indicating the formation of Fe_3O_4 nanoparticles. After a fixed time (varying between 0 and 10 min), the diazonium salt (0.5 mmol) synthesized above was added directly into the reaction vessel. The mixture was stirred for 1 h. The particles were then washed by 7 cycles of centrifugation/redispersion (using an ultrasonic bath during 15 min) in water and ethanol and dried at 40 °C. The IR analysis (given in the Supporting Information (SI)) of the products obtained after each washing cycle gave evidence of the necessity to perform up to 5 cycles of centrifugation/redispersion in order to release all of the loosely bound molecules from the NP surface. Their X-ray diffraction (XRD) patterns (see Figure SI-2, in the SI)

Received: October 13, 2010
Published: January 19, 2011

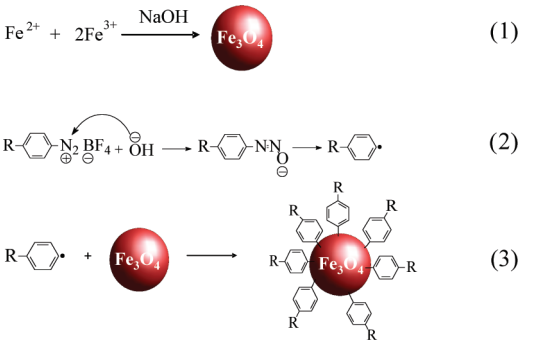

Figure 1. *In situ* surface functionalization of Fe_3O_4 NPs by 2-hydroxyethylphenyldiazoate species.

Table 1. Summary of the Diameters of NP-C_6H_4-$(CH_2)_2$-OH Particles Obtained by Varying the Time of Introduction of BF_4, N_2-C_6H_4-$(CH_2)_2$-OH in the Synthesis Medium

Time[a] (min)	$\langle D_{TEM}\rangle$ (nm)	$\langle L_{XRD}\rangle$ (nm)	$(\langle \varepsilon^2\rangle)^{1/2}$	Organic shell (mass %)	IR $\delta_{C=C}$ band at 1600 cm^{-1}
b	10.5 ± 0.6	10.6	1×10^{-3}	4	Nonvisible
0	7.3 ± 0.5	8.7	1×10^{-4}		Intense
5	9 ± 0.5	8.6	7×10^{-4}		medium
10	10 ± 0.7	10.1	3×10^{-4}	20	medium

[a] Time elapsed before the introduction of the diazonium salt. [b] Without added diazonium salt.

are characteristic of the spinel phase with broadened peaks. The cell parameter, the size of the coherent diffraction domain ($\langle L_{XRD}\rangle$), and the average lattice formation due to microstrains ($(\langle \varepsilon^2\rangle)^{1/2}$) were determined with MAUD software[15,16] which is based on the Rietveld method combined with Fourier analysis. First, the refined average crystal size and cell parameter agree well with the formation of nanocrystalline magnetite. Second, the crystal size appears to be dependent on the presence of the diazonium salt or its absence in the reaction medium and seems to be affected by the time elapsed before its introduction (see Table 1).

Clearly, the coating limits the crystalline growth particularly when the salt is introduced at the beginning of the reaction ($t = 0$ min). Note that, after 10 min of reaction, the introduction of the diazonium salt has no more effect on the particle size since the measured sizes are close to that obtained in the absence of the salt. Transmission electron microscopy (TEM) showed particles with close to spherical shapes, almost uniform in size with an average particle diameter ($\langle D_{TEM}\rangle$) of 10 nm (standard deviation of about 10%) depending on the introduction time of the diazonium salt in the starting solution (Table 1). Figure 2a illustrates this result in the case of the NP-C_6H_4-$(CH_2)_2$-$OH_{t=0}$ particles (the salt is introduced at t = 0 min) which exhibit a diameter decrease of 3 nm (*ca.* 20%) by comparison with the NPs synthesized in the absence of the diazonium salt.

It is noteworthy that the NPs do not appear very well separated from each other on the TEM images, probably due to the low thickness of the aryl layer coating. Nevertheless, by zooming on the TEM images (see SI-3 in SI), a tight separation between each NP could be evidenced, indicative of a nonaggregated state. The proximity between sizes inferred from XRD and TEM analysis, respectively, suggests that the

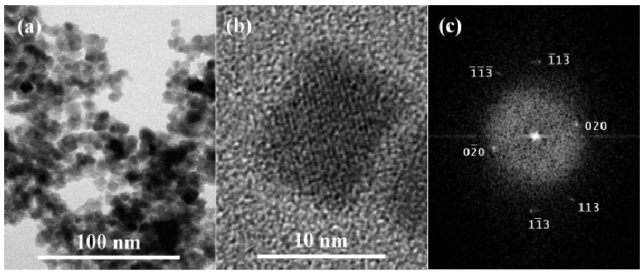

Figure 2. Transmission electron micrograph showing NP-C_6H_4-$(CH_2)_2$-$OH_{t=0}$ particles (a). High-resolution transmission electron micrograph showing a highly crystalline and faceted particle (b) with its FFT pattern (c).

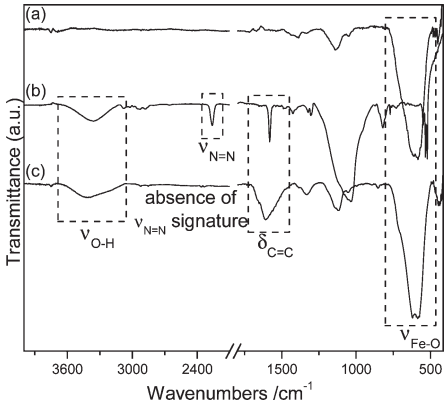

Figure 3. FT-IR spectra of (a) bare Fe_3O_4 NPs; (b) $BF_{4,2}$N-C_6H_4-$(CH_2)_2$-OH; and (c) NP-C_6H_4-$(CH_2)_2$-$OH_{t=0}$.

produced particles are single crystals. To confirm that, high resolution (HRTEM) images were recorded (see Figure 2b). They show that the particles are faceted single crystals with not exactly a spherical but much more of a polygonal shape and with fringes corresponding to crystallographic planes of the cubic lattice of the spinel structure. From the core to the surface of the crystal there is no evidence of defects such as dislocations or stacking faults, but at the surface a thin amorphous shell appears suggesting a surface disorder probably due to the formation of Fe_3O_4−aryl surface bonds. The diffraction pattern (Figure 2c) calculated from the high resolution image of the particle core corresponds to the (311) and (200) planes of the magnetite phase with a cell parameter of 8.40 Å.

Figure 3 allows comparison of the IR spectra of free BF_4, N_2-C_6H_4-$(CH_2)_2$-OH (Figure 3b), bare Fe_3O_4 particles (Figure 3a), and the products of the reaction between these two species, NP-C_6H_4-$(CH_2)_2$-$OH_{t=0}$ nanoparticles (Figure 3c). Bare NPs display one intense characteristic band at 550 cm^{-1}, due to Fe−O stretching vibrations.

The IR spectrum of the free diazonium salt is characterized by three strong bands in the 3500−1500 cm^{-1} region: ν_{O-H} at 3300 cm^{-1}, $\nu_{N\equiv N}$ at 2280 cm^{-1}, and $\delta_{C=C}$ at 1680 cm^{-1}. The spectrum of NP-C_6H_4-$(CH_2)_2$-$OH_{t=0}$ nanoparticles appears to be a combination of the spectra of pure NPs (band at 550 cm^{-1}) and of the hydroxyethylphenyl moieties (bands at 3300 and 1680 cm^{-1}), confirming the presence of a hydroxyethylphenyl coating on the Fe_3O_4 particles. Yet, the most striking difference is the disappearance of the N≡N stretching mode near 2280 cm^{-1} in NP-C_6H_4-$(CH_2)_2$-$OH_{t=0}$ particles, indicating the release of N_2 as a consequence of the cleavage of the diazonium moieties.

dx.doi.org/10.1021/ja108928b |*J. Am. Chem. Soc.* 2011, 133, 1646–1649

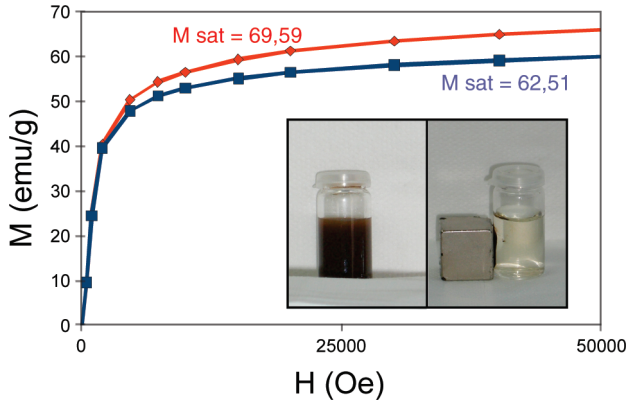

Figure 4. 5K-First magnetization of the Fe_3O_4 particles (red line) compared to that of NP-C_6H_4-$(CH_2)_2$-$OH_{t=0}$ nanoparticles (blue line). In the box are shown numerical photographs of the aqueous colloids in the absence (left) and presence (right) of a permanent magnet.

The magnetizations of bare Fe_3O_4 particles and aryl-coated ones were measured as a function of the magnetic field at low temperature (5 K) on a SQUID magnetometer. Figure 4 shows that it is hardly affected by the surface modification. A magnetization reduction of about 10% is observed between uncoated and coated particles. It is clearly related to (1) the decrease in NP size, (2) the increased surface disorder, and (3) the diamagnetic contribution of aryl species. This decrease remains quite weak and must not seriously affect further use of these particles in the desired applications.

Like other monolayer-protected nanoparticles, the NP-C_6H_4-$(CH_2)_2$-OH were soluble not only in apolar organic solvents such as dichloromethane, THF, toluene, and chloroform but also in polar solvents such as methanol and ethanol or water (see Figure 4).

The thermal and decomposition characteristics of the materials were determined by thermal gravimetric analyses, in the temperature range 20−800 °C with a heating rate of 10 °C/min under a flow of air at 80 mL/min. A total weight loss of 20% was observed on heating aryl-coated Fe_3O_4 NPs to 800 °C while the uncoated NPs showed a weight loss of only 4% (probably due to some contamination species). This result suggests a high grafting density of the aryl group on the nanoparticle surface. Taking into account the average particle diameter D(NP-C_6H_4-$(CH_2)_2$-$OH_{t=0}$) = 10.0 nm of a single unfunctional particle obtained from TEM, and the density of Fe_3O_4, which is 5.2 $g \cdot cm^{-3}$, a specific surface area of 115 $m^2 \cdot g^{-1}$ is obtained which yields a surface coverage Γ of 0.8×10^{19} aryl molecules $\cdot m^{-2}$. It is noteworthy that this value is on the same order of magnitude as the surface concentration of a close-packed monolayer Γ_{CPML} of phenyl (or 4-substituted phenyl) groups estimated from molecular models.[17]

The mechanism for the grafting reaction involves the formation of diazoate species in a basic medium,[12] which dediazonize (with a half-life of ~1750 s) along a homolytic pathway to give the aryl radicals.[18] These aryl radicals react with the Fe_3O_4 NPs during their formation and stop their growth. In order to extend this functionnalization strategy to NPs that cannot be synthesized at room temperature in aqueous media, we studied whether it could be applied in a postfunctionalization step. Fe_3O_4 NPs were first prepared by hydrolysis of iron acetate salts (0.2 M) in diethyleneglycol (125 mL) under reflux for at least 6 h and washed by seven cycles of centrifugation/redispersion. The particles (100 mg) were then dispersed in a basic aqueous solution ([NaOH] = 0.1 M) in which was added the diazonium salt (0.5 mM). After 20 min, the particles were washed and dried. The IR spectrum (displayed in the SI, Figure SI-4) of the NPs prepared by this two-step strategy is very similar to that obtained previously after the one-pot synthesis, evidencing the grafting of the aryl group layer at the surface of the NPs.

In summary, we have presented an original and simple route to synthesize water-soluble magnetite nanocrystals by room temperature hydrolysis of iron chloride salts in alkaline water and in the presence of a diazonium salt. Differently sized magnetite nanocrystals can be obtained simply by varying the introduction time of the diazonium salt in the starting solution. Furthermore, preformed NPs could be postfunctionalized by diazonium salt treatment, with the same derivatization efficiency. We believe that this novel synthetic approach will not only pave a new way for the preparation of water-soluble magnetite nanocrystals but also provide a general functionalization strategy for magnetic nanoparticles.

■ ASSOCIATED CONTENT

Supporting Information. Material synthesis, experimental procedures, and complementary characterization results. This material is available free of charge via the Internet at http://pubs.acs.org.

■ AUTHOR INFORMATION

Corresponding Author
mangeney@univ-paris-diderot.fr

■ REFERENCES

(1) (a) Chin, S. F.; Makha, M.; Raston, C. L.; Sanders, M. *Chem. Commun.* **2007**, *19*, 1948–1950. (b) Klokkenburg, M.; Vonk, C.; Claesson, E. M.; Meeldijk, J. D.; Erné, B. H.; Philipse, A. P. *J. Am. Chem. Soc.* **2004**, *126*, 16706–16707.

(2) (a) Wan, J.; Cai, W.; Meng, X.; Liu, E. *Chem. Commun.* **2007**, 5004–5006. (b) Choi, J.; Lee, J. H.; Shin, T. H.; Song, H. T.; Kim, E. Y.; Cheon, J. *J. Am. Chem. Soc.* **2010**, *132*, 11015–11017.

(3) (a) Thierry, B.; Al-Ejeh, F.; Khatri, A.; Yuan, Z.; Russell, P. J.; Ping, S.; Brown, M. P.; Majewski, P. *Chem. Commun.* **2009**, *47*, 7348–7350. (b) Thomas, C. R.; Ferris, D. P.; Lee, J. H.; Choi, E.; Cho, M. H.; Kim, E. S.; Stoddart, J. F.; Shin, J. S.; Cheon, J.; Zink, J. I. *J. Am. Chem. Soc.* **2010**, *132*, 10623–10625.

(4) (a) Milone, C.; Ingoglia, R.; Schipilliti, L.; Crisafulli, C.; Neri, G.; Galvagno, S. *J. Catal.* **2005**, *236*, 80–90. (b) Ling, M. M.; Wang, K. Y.; Chung, T. S. *Ind. Eng. Chem. Res.* **2010**, *49*, 5869–5876.

(5) (a) Tadmor, R.; Rosensweig, R. E.; Frey, J.; Klein, J. *Langmuir* **2000**, *16*, 9117–9120. (b) Rosensweig, R. E.; Kaiser, R.; Miskolczy, G. *J. Colloid Interface Sci.* **1969**, *29*, 680–686.

(6) Rockenberger, J.; Scher, E. C.; Alivisatos, A. P. *J. Am. Chem. Soc.* **1999**, *121*, 11595–11596.

(7) Yee, C.; Kataby, G.; Ulman, A.; Prozorov, T.; White, H.; King, A.; Rafailovich, M.; Sokolov, J.; Gedanken, A. *Langmuir* **1999**, *15*, 7111–7115.

(8) (a) Lu, J.; Fan, J.; Xu, R.; Roy, S.; Ali, N.; Gao, Y. *J. Colloid Interface Sci.* **2003**, *258*, 427–431. (b) Kataby, G.; Ulman, A.; Prozorov, R.; Gedanken, A. *Langmuir* **1998**, *14*, 1512–1515.

(9) (a) Dahoumane, S. A.; Nguyen, M. N.; Thorel, A.; Boudou, J. P.; Chehimi, M. M.; Mangeney, C. *Langmuir* **2009**, *25*, 9633–9638. (b) Matrab, T.; Save, M.; Charleux, B.; Pinson, J.; Cabet-Deliry, E.; Adenier, A.; Chehimi, M. M.; Delamar, M. *Surf. Sci.* **2007**, *601*, 2357–2366. (c) Matrab, T.; Chancolon, J.; Mayne-L'Hermite, M.; Rouzaud, J. N.;

Deniau, G.; Boudou, J. P.; Chehimi, M. M.; Delamar, M. *Colloids Surf., A* **2006**, *287*, 217–221. (d) Bahr, J. L.; Yang, J.; Kosynkin, D. V.; Bronikowski, M. J.; Smalley, R. E.; Tour, J. M. *J. Am. Chem. Soc.* **2001**, *123*, 6536–6542. (e) Doyle, C. D.; Rocha, J.-D. R.; Weisman, R. B.; Tour, J. M. *J. Am. Chem. Soc.* **2008**, *130*, 6795–6800. (f) Price, B. K.; Tour, J. M. *J. Am. Chem. Soc.* **2006**, *128*, 12899–12904. (g) Mangeney, C.; Qin, Z.; Dahoumane, S. A.; Adenier, A.; Herbst, F.; Boudou, J. P.; Pinson, J.; Chehimi, M. M. *Diamond Relat. Mater.* **2008**, *17*, 1881–1887. (h) Mahouche Chergui, S.; Ledebt, A.; Mammeri, F.; Herbst, F.; Carbonnier, B.; Ben Romdhane, H.; Delamar, M.; Chehimi, M. M. *Langmuir* **2010**, *26*, 16115–16121.

(10) (a) Mirkhalaf, F.; Paprotny, J.; Schiffrin, D. J. *J. Am. Chem. Soc.* **2006**, *128*, 7400–7401. (b) Kumar, V. K. R.; Gopidas, K. R. *Chem. Asian J.* **2010**, *5*, 887–896. (c) Ghosh, D.; Chen, S. *J. Mater. Chem.* **2008**, *18*, 755–762. (d) Shengnan, Y.; Qinmin, P.; Liu, J. *Electrochem. Commun.* **2010**, *12*, 479–482. (e) Ghosh, D.; Pradhan, S.; Chen, W.; Chen, S. *Chem. Mater.* **2008**, *20*, 1248–1250.

(11) (a) Maldonado, S.; Smith, T. J.; Williams, R. D.; Morin, S.; Barton, E.; Stevenson, K. J. *Langmuir* **2006**, *22*, 2884–2891. (b) Hurley, B. L.; McCreery, R. L. *J. Electrochem. Soc.* **2004**, *151*, 252–259.

(12) Hegarty, A. F. In *The Chemistry of Diazonium and Diazo Groups*, Part 2; Patai, S., Ed.; John Wiley and Sons: 1978; p 511.

(13) Combellas, C.; Kanoufi, F.; Pinson, J.; Podvorica, F. I. *Electrochim. Acta* **2009**, *54*, 2164–2170.

(14) Gam-Derouich, S.; Nguyen, M. N.; Madani, A.; Maouche, N.; Lang, P.; Perruchot, C.; Chehimi., M. M. *Surf. Interface Anal.* **2010**, *42*, 1050–1056.

(15) Lutterotti, L; Matthies, S; Wenk, H. R. *Newsletter of the Commission on Powder diffraction* **1999**, *21*, 14–15.

(16) The profile of the diffraction peaks of all the samples was refined by a Pseudo-Voigt function where the contribution of $(\langle \varepsilon^2 \rangle)^{1/2}$ to peak-broadening is Gaussian while that of finite crystal size $\langle R \rangle$ is Lorentzian. This analysis shows that the $(\langle \varepsilon^2 \rangle)^{1/2}$ values are very weak suggesting that the powders consist of almost strain-free nanocrystals.

(17) Pinson, J.; Podvorica, F. *Chem. Soc. Rev.* **2005**, *34*, 429–439.

(18) Pazo-Llorente, R.; Bravo-Diaz, C.; Gonzalez-Romero, E. *Eur. J. Org. Chem.* **2004**, *15*, 3221–3226.